GSSC 武漢理工大學 绿色智能江海直达船舶与邮轮游艇研究中心 Green & Smart River-Sea-Going Ship Cruise and Yacht Research Center

Research On Decarbonization And Frictional Resistance Reduction With Microbubble Drag Reduction

YANAN ZHOU, ZHIYONG PEI, GUANGWU LIU, MIRKO TOMAN

Wuhan University of Technology

Siemens Digital Industry Software

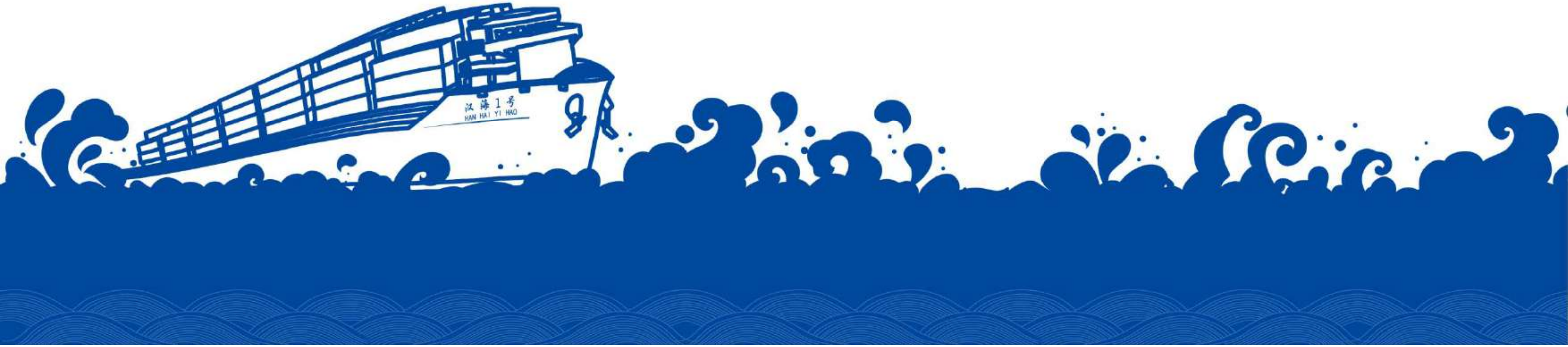

CONTENTS

Introduction

Introduction

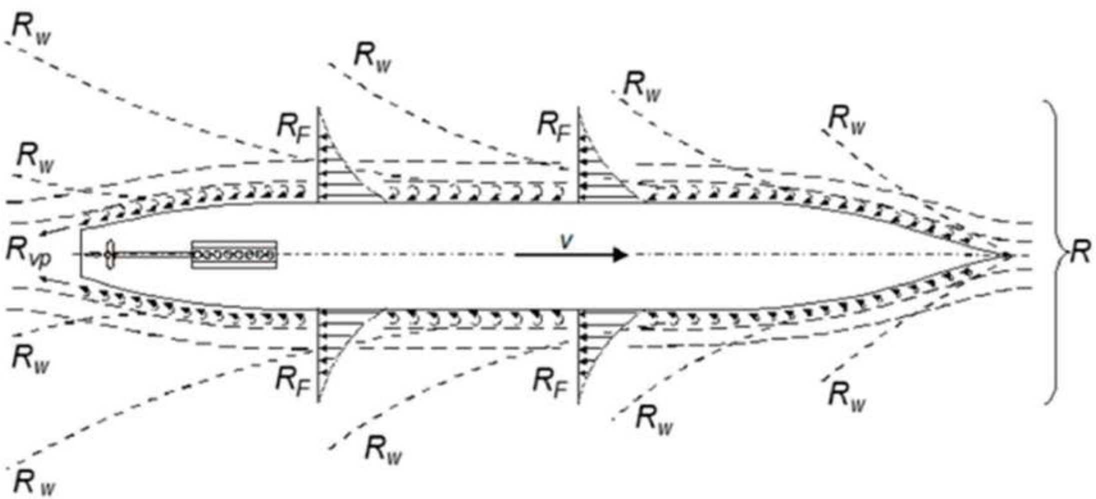

$$R = R_f + R_{pv} + R_w$$

Low-speed Ship: friction resistance is as high as 70~80%

High-speed Ship: friction resistance is about 50%

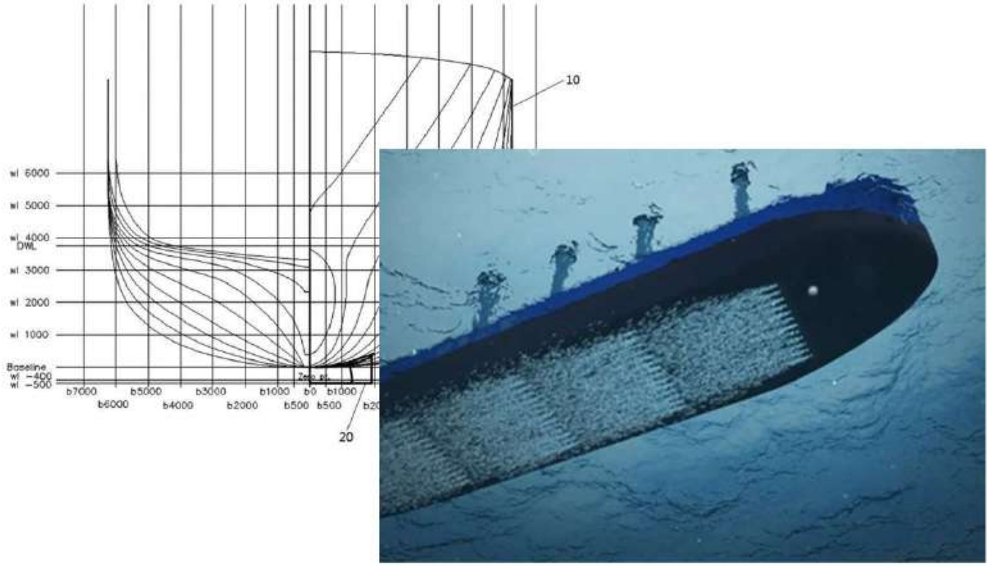

MBDR is one of the most promising drag reduction techniques.

Introduction

Froude

Injecting gas between the ship hull and water alters viscosity and density, aiming to reduce friction resistance.

Merkle et.al

- The mechanism of turbulent boundary layer is central to the solution of microbubble drag reduction.
- Optimizing the flow of microbubbles can be achieved by controlling the size and trajectory of microbubbles.

Elbing et.al

A blend of microbubble and air layers results in a mixture, where resistance reduction varies linearly with airflow rate.

Introduction

Sato et.al

Towing tests on a ship model found a maximum friction reduction of about 30% and a maximum effective power saving of 14.7%.

Mizokami et.al

Baffle helped to equalize the air distribution and effectively reduced the drag of the model.

Gunawa et.al

Positioning the jet nozzle slightly aft on the bow improved drag reduction by increasing microbubble coverage.

Taiji et.al

Increased microbubble flow reduces ship bottom friction, achieving up to 28% overall drag reduction and 50% local drag reduction.

Mechanism of Microbubble Drag Reduction

Mechanism of Microbubble Drag Reduction

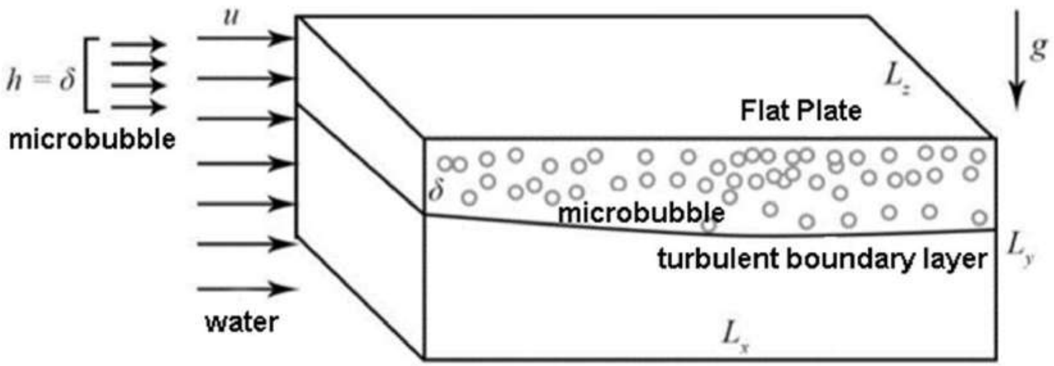

Fluid flow follows the laws of conservation of mass and conservation of momentum.

Continuity Equation:

$$\frac{\partial u}{\partial x}+\frac{\partial v}{\partial y}+\frac{\partial w}{\partial z}=0$$

Motion equation:

$$\frac{\partial \rho u}{\partial t}+div(\rho u u)=-\frac{\partial p}{\partial x}+\frac{\partial \tau_{xx}}{\partial x}+\frac{\partial \tau_{yx}}{\partial y}+\frac{\partial \tau_{zx}}{\partial z}+F_x$$

$$\frac{\partial \rho v}{\partial t}+div(\rho v u)=-\frac{\partial p}{\partial y}+\frac{\partial \tau_{xy}}{\partial x}+\frac{\partial \tau_{yy}}{\partial y}+\frac{\partial \tau_{zy}}{\partial z}+F_y$$

$$\frac{\partial \rho w}{\partial t}+div(\rho w u)=-\frac{\partial p}{\partial z}+\frac{\partial \tau_{xz}}{\partial x}+\frac{\partial \tau_{yz}}{\partial y}+\frac{\partial \tau_{zz}}{\partial z}+F_z$$

- Mixture Model
- Eulerian-Eulerian Model
- Eulerian-Lagrangian Model

Eulerian-Lagrangian Model

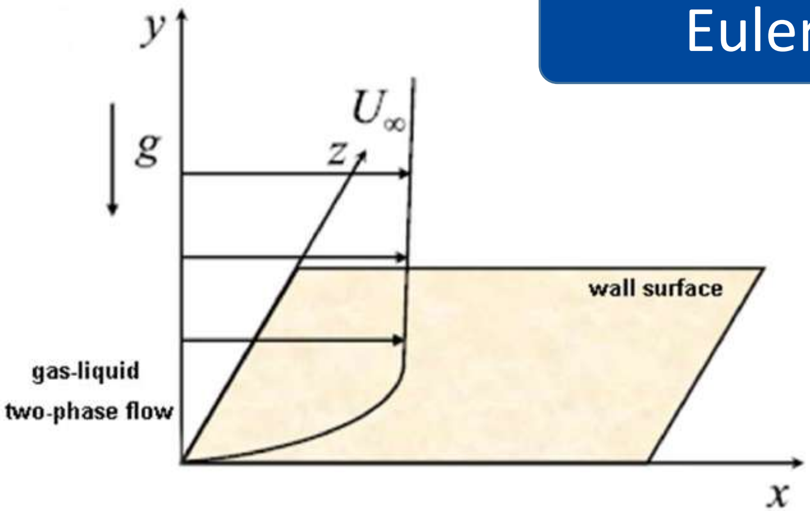

$$F_B = F_d + F_l + F_{v.m} + F_{t.d} + F_{w.l}$$

$$F_B = m_B \frac{dv_B}{dt}$$

$$x_B^{n+1} = x_B^n + V_{xB}^n \Delta t$$

Water--Continuous phase

Microbubble--Dispersed phase

Analyzing the motion trajectory of microbubbles to describe the movement of the dispersed phase.

Mechanism of Microbubble Drag Reduction

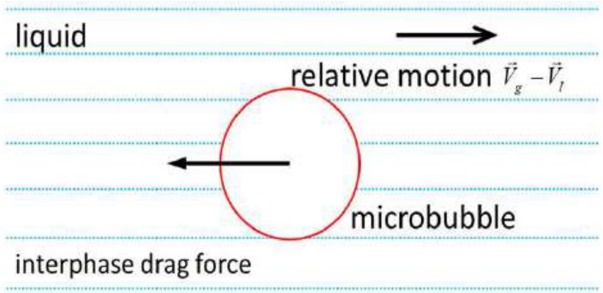

$$F_d = 0.75\eta_a C_d \frac{\rho_f}{d_a}\left|v_f - v_a\right|\left(v_f - v_a\right)$$

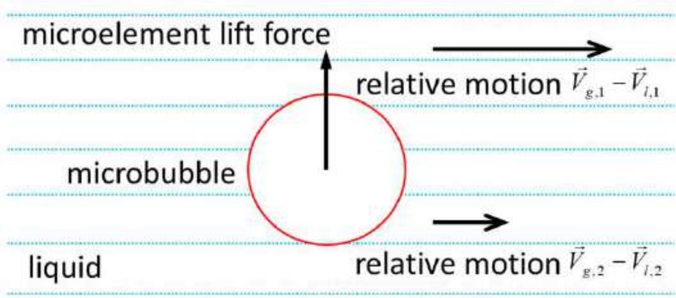

$$F_l = \eta_a \rho_f C_l \left(v_a - v_f\right) \times \nabla \times v_f$$

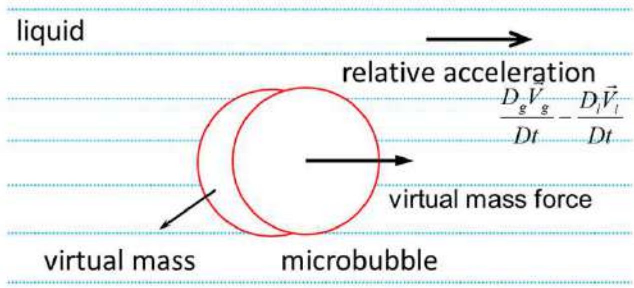

$$F_{v.m} = \frac{C_{v.m}}{12} d_B^3 \rho_f \left(\frac{dv_f}{dt} - \frac{dv_B}{dt}\right)$$

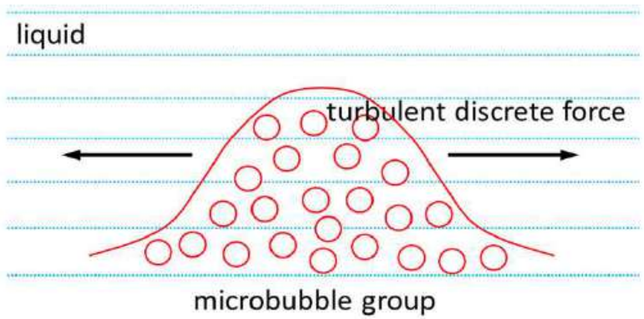

$$F_{t.d} = -\rho_f E_f \nabla \eta_a$$

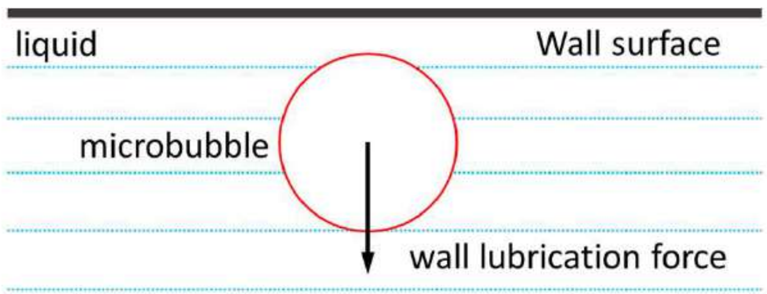

$$F_{w.l} = C_{w.l}\eta_a \rho_f \left|v_a - v_f - \left[\left(v_a - v_f\right)\cdot n\right]n\right| n$$

Microbubble Drag Reduction Test System

Microbubble Drag Reduction Test System

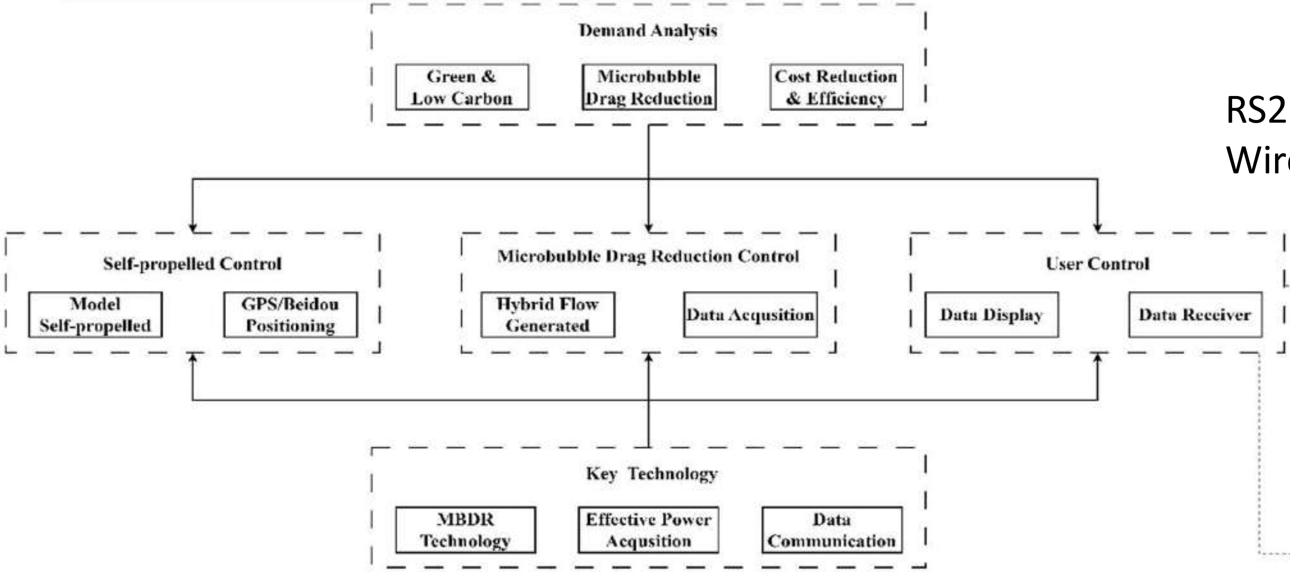

RS232 protocol for intra-module data transmission.
Wireless communication for inter-unit data transmission.

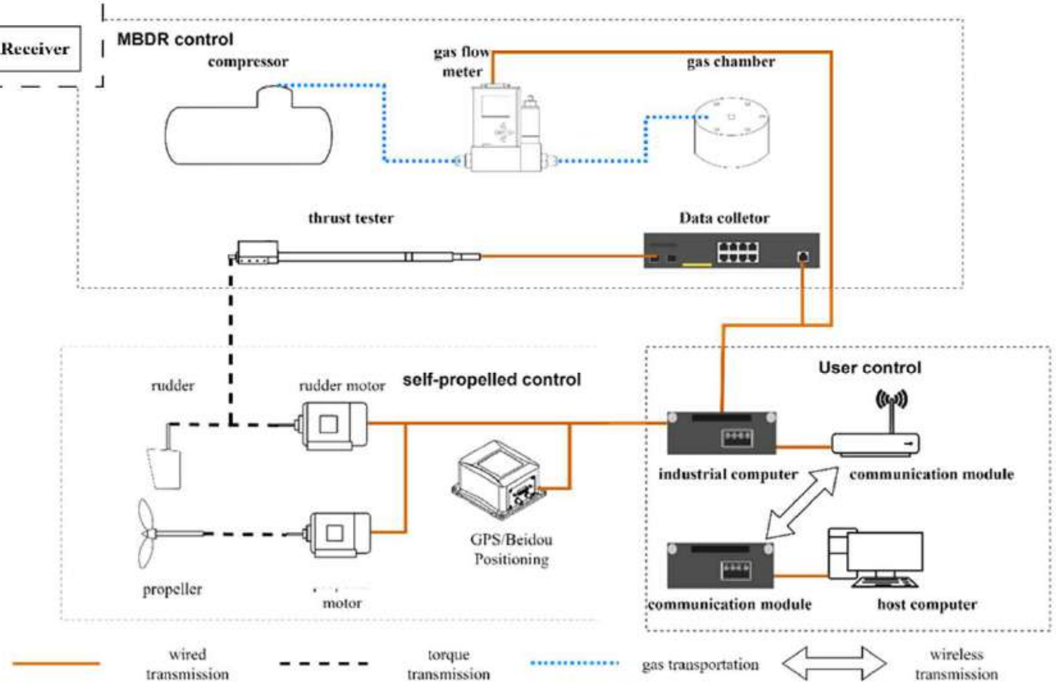

Focus on Green & Low Carbon, Microbubble Drag Reduction (MBDR), cost-effectiveness.
Using MBDR Technology ,Effective Power Acquisition, Data Communication
Comprised a Self-propelled Control Unit, MBDR Control Unit, User Control Unit.

Microbubble Drag Reduction Test System

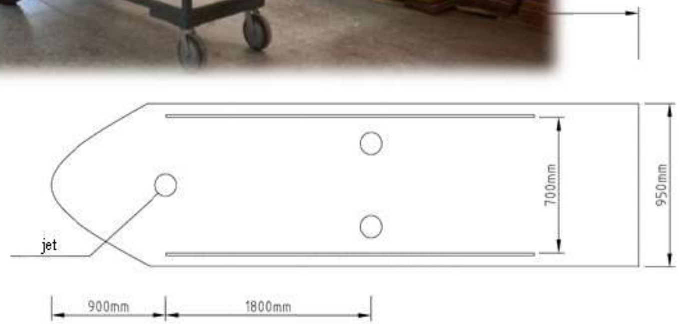

The test utilizes the 1140TEU River-Sea Going Ship as the prototype. A test model is fabricated with a scaling ratio of 1:25 for accurate representation in experimental conditions

The test speed was similarly determined by Froude number (F_r) to be 11.5 knots for the design speed of the 1140 TEU River-Sea-Going Ship.
The gas flow rate in the range of 0 to 1 SLM In order to investigate the airflow rate magnitude of MBDR, the dimensionless airflow rate coefficient C_Q is defined.

	1140 TEU ship	Model
L_{OA}	139.8m	5.5m
B	26.0m	0.95m
d	6.5m	0.255m

V (m/s)	0.58、0.69、0.75、0.84、0.92、0.99
Fr	0.079、0.094、0.102、0.114、0.125、0.135
Q (SLM)	0~1.0SLM
C_Q	0.001284~0.01958

Microbubble Drag Reduction Test System

- unconstrained self-propelled tests were conducted in the maneuvering pool.
- propelled to the target speed， recorded the real-time thrust once stability was achieved.
- the value of the model's thrust can be regarded as the value of drag force
- adjusting parameters to gather MBDR data for the model at different speeds and microbubble rates.

Microbubble Adaptive Control Technology

Gas Flow Adaptive Control Technology

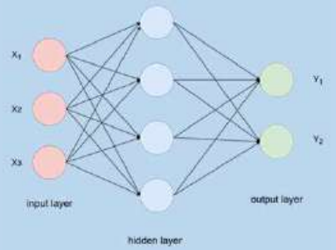

The BP Neural Network primarily comprises loss forward propagation and error backpropagation.

calculates the loss between the output function and the objective function

transfers the output to the input, obtain the errors of each unit

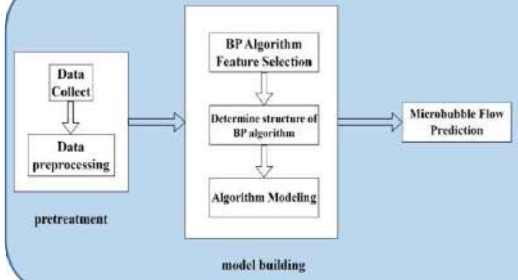

The database for the BP Neural Network model is derived from self-propelled model test.

Focuses on : Speed, Microbubble Flow Rate, Thrust.

The neuron network topology of BP Neural Network model structure is 1-9-13-1.

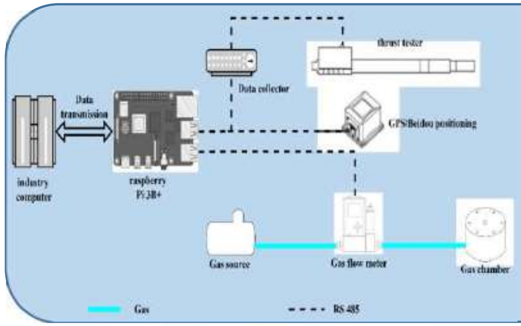

Raspberry Pi 3B+ :executing the BP Neural Network and regulating the microbubble flow based on real-time thrust and air state data.

thrust acquisition module : measuring propeller thrust data

flow control meter: adjusting gas flow according to commands from the control unit.

Gas Flow Adaptive Control Technology

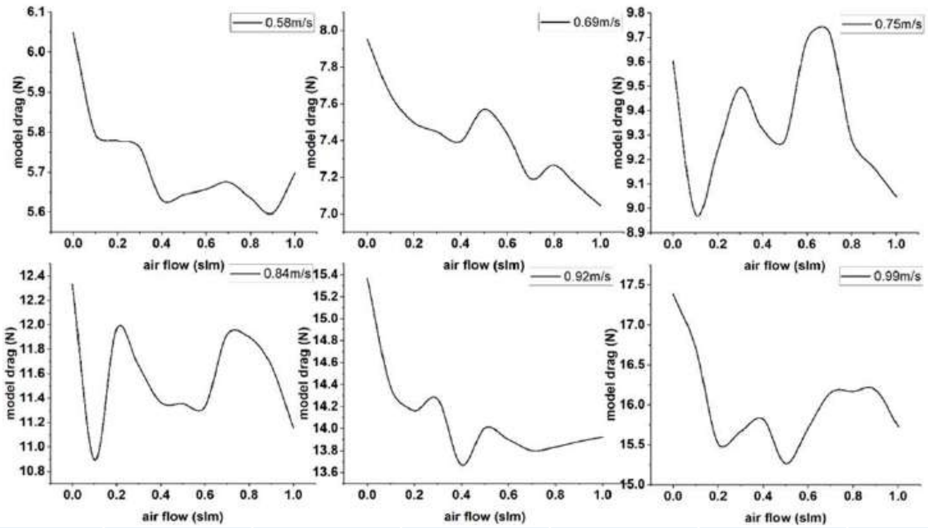

	0.58	0.69	0.75	0.84	0.92	0.99
OMFR (SLM)	0.9	1	0.1	0.1	0.4	0.5

Microbubble drag reduction effectively reduces the sailing resistance.
Specific microbubble flow rate minimizes the sailing resistance of different test model.

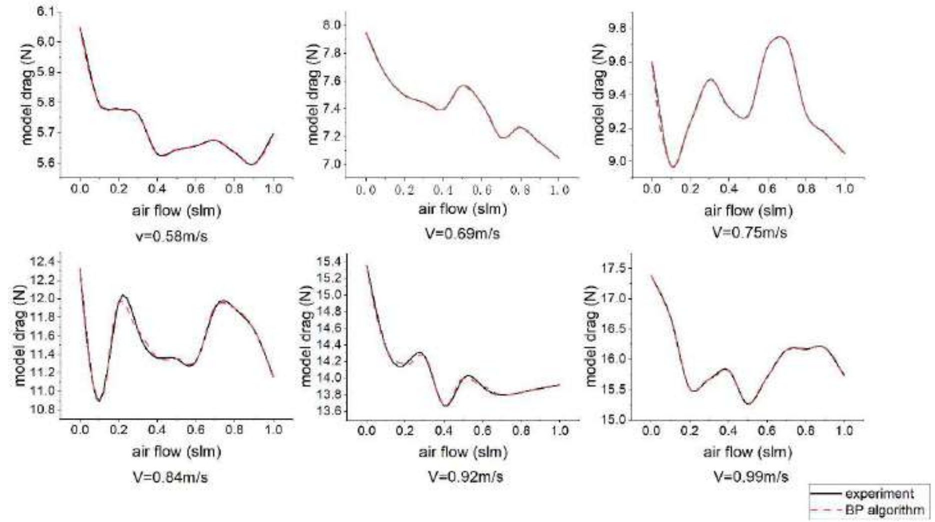

Utilizing this test data as a sample, the resistance of the model was calculated by using a 4-layer BP neural network algorithm. Obtaining the data for resistance under a specific speed and various microbubble flow rates.

Gas Flow Adaptive Control Technology

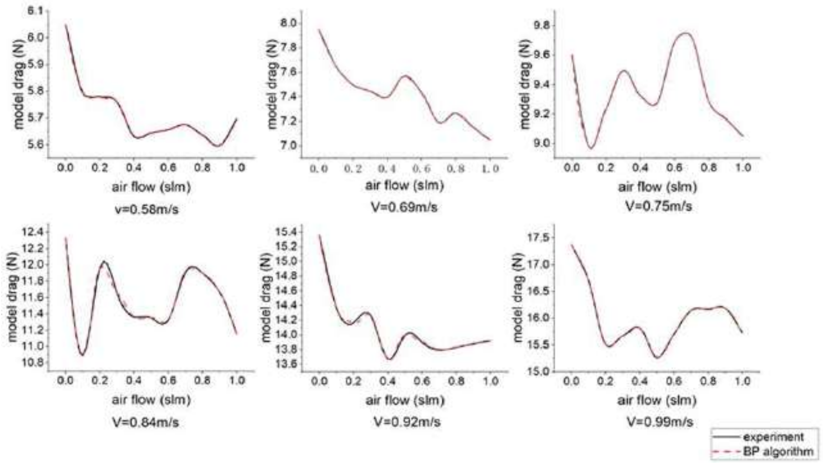

	350	400	450	500	550	600
MSE	3.21×10-6	1.23×10-5	1.59×10-5	8.3×10-5	3.04×10-5	7.35×10-5
MMSE	1.04×10-6	8.79×10-6	1.03×10-5	5×10-5	1.88×10-5	4.07×10-5

- Calculating the error between the iterative calculation and the OMFR in the test data.
- The predictive model has good data accuracy.

	0.58m/s	0.69m/s	0.75m/s	0.86m/s	0.92m/s	0.99m/s
1	0.88	1	0.12	0.1	0.41	0.5
2	0.88	1	0.12	0.1	0.41	0.5
3	0.88	1	0.12	0.11	0.41	0.5
4	0.88	1	0.11	0.1	0.41	0.5
5	0.88	1	0.12	0.11	0.41	0.5
6	0.88	1	0.11	0.1	0.41	0.5
7	0.88	1	0.11	0.1	0.41	0.51
8	0.88	1	0.12	0.11	0.41	0.5
9	0.88	1	0.12	0.11	0.41	0.5
10	0.88	0.99	0.12	0.11	0.41	0.5

- Using genetic algorithm optimization operation obtaining the OMFR.
- Combining BP neural network with genetic algorithm has high stability.

Conclusion

Conclusion

Basement

Focus	Application of microbubble drag reduction technology to River-Sea-Going ships.
Data	Self-propelled tests were conducted to gather data on model thrust and microbubble flow rate.
System	Combining BP neural network and genetic algorithm, developing based on the collected data.

Conclusion

Method

Predict

predicting optimal microbubble flow rates under various conditions, and its accuracy and stability were verified through simulation.

Impact

speed and microbubble flow rate significantly affects microbubble drag reduction technology and ship resistance.

Relationship

Microbubble flow rate and model resistance exhibit a complex nonlinear relationship at a given speed.

Conclusion

Result

Achievement

Predicting optimal microbubble flow rates under various conditions, and its accuracy and stability were verified through simulation.

Advantage

The development of this system enhances the accessibility and usability of microbubble drag reduction technology, making its application more feasible.

3D Plate Cold Bending Machine

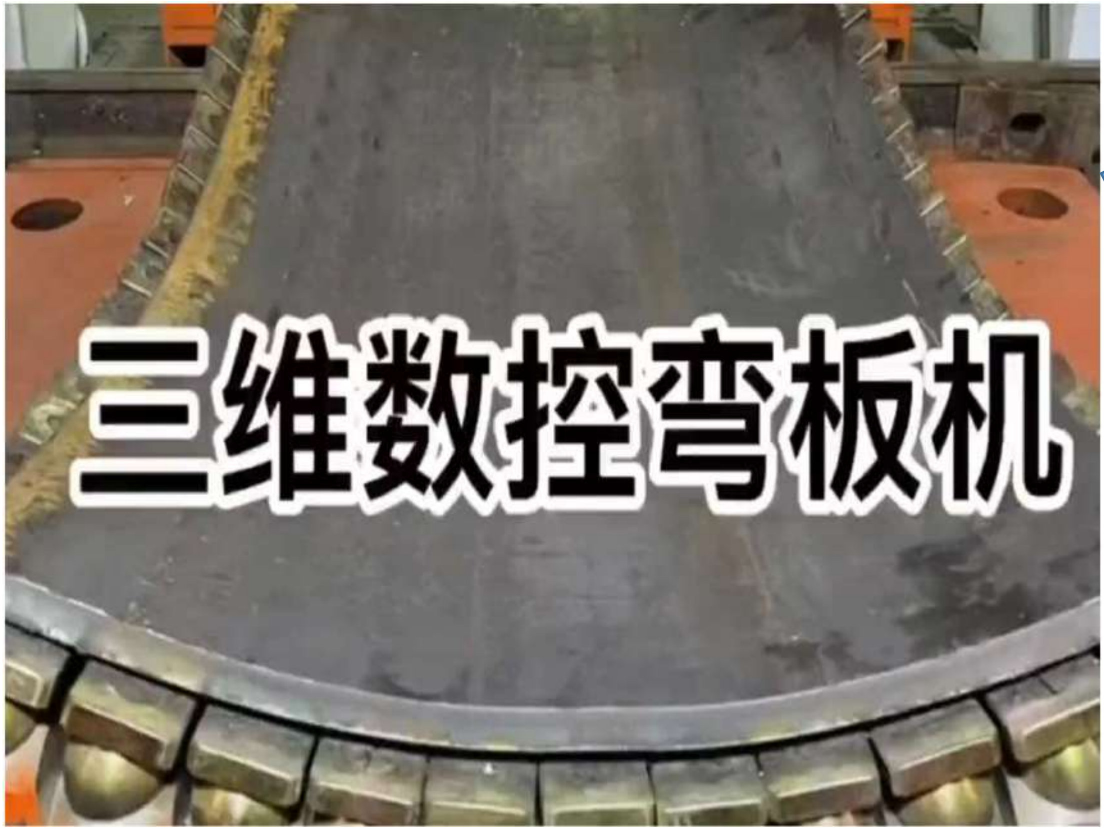

Sail-Shaped

Saddle-Shaped

Other Curve

Traditional Processing: Cold Pressing + Line Heating Operation

PROBLEMS
- Bad working Environment
- Pollution
- Low forming precision
- Low efficiency
- Piece drawbacks

Traditional workflow

BENEFITS

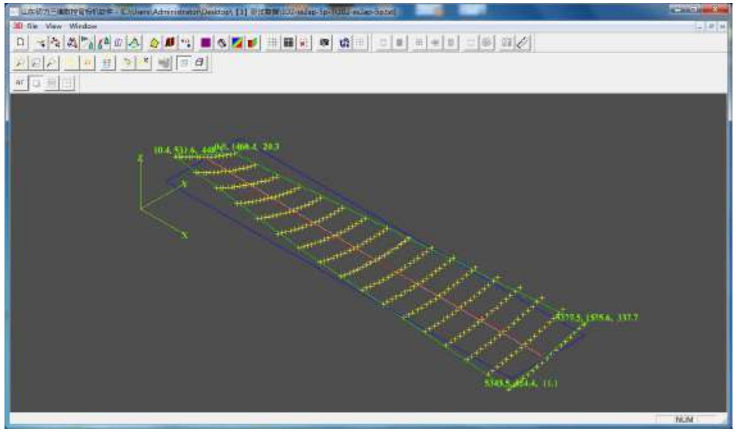

- ✓ No line heating
- ✓ Accurate forming
- ✓ High efficiency (10 times + faster)
- ✓ No piece damage
- ✓ Automatic data transfer
- ✓ Environment friendly


Europäisches Patentamt
European Patent Office
Office européen des brevets

URKUNDE | CERTIFICATE | CERTIFICAT

It is hereby certified that a European patent has been granted in respect of the invention described in the patent specification for the Contracting States designated in the specification.

2487257

Taian Suncle Hydraulic Equipments Manufactory
Nanshanggao Village
Shanggao Town
Taishan
Tai'an
Shandong 271000/CN

20.11.13

武漢理工大學
绿色智能江海直达船舶与邮轮游艇研究中心
Green & Smart River-Sea-Going Ship Cruise and Yacht Research Center

Thanks

CONTACT

Guangwu Liu

+86 13917089848 (WhatsApp)

gliu@whut.edu.cn

www.linkedin.com/in/gwliu

www.whut.edu.cn